Proceedings of the
7th Graz Brain-Computer Interface Conference 2017 DOI: 10.3217/978-3-85125-533-1-52

ERROR-RELATED POTENTIALS WITH MASKED AND UNMASKED ONSET DURING CONTINUOUS CONTROL AND FEEDBACK

C. Lopes Dias[1], A. I. Sburlea[1], G. R. Müller-Putz[1]

[1]Institute of Neural Engineering, Graz University of Technology, Graz, Austria

E-mail: gernot.mueller@tugraz.at

ABSTRACT: Brain-computer interfaces (BCIs) are prone to errors in the decoding of the user's intention, yet the detection of errors can be used to improve the performance of BCIs. We recorded the EEG data of 8 subjects who participated in an experiment to study error-related potentials (ErrPs) with masked and unmasked onset, during a task with continuous control and continuous feedback. The masked ErrPs had a delayed onset and less pronounced peak amplitudes when compared to the unmasked ErrPs. We obtained an average classification rate of 94% for correct trials and of 80% for error trials. The classification rates for masked errors against unmasked errors were at chance level.

INTRODUCTION

Brain-computer interfaces (BCIs) provide control to their users, by recognising their intention from neuronal activity [1]. BCIs are susceptible to errors in the decoding of the user's intention and benefit from the ability to detect what the user perceives as erroneous in order to improve performance. This is possible because the recognition of an error elicits a neuronal response that is associated with a coarse differentiation between favorable and unfavorable outcomes [2] and that can be measured using various techniques, e.g. electroencephalography (EEG). The electrophysiological signature of error detection is named error-related potential (ErrP) and is obtained by subtracting the averaged electrophysiological trace following correct events from the averaged trace following erroneous events.

Different types of ErrPs have been described in literature [3]: response ErrPs occur in speeded response time tasks in which subjects are asked to respond as quickly as possible to a stimulus; observation ErrPs occur when subjects observe an error being committed by an external agent; feedback ErrPs occur when subjects receive the information that the action they performed was not correct; and interaction ErrPs occur in the context of BCIs, when users believe that the command they issued was misinterpreted by the interface.

In BCIs that are controlled in a discrete way, the occurrence of interaction ErrPs is well established [4, 5]. In this context, interaction ErrPs can be detected on a single-trial basis [5, 6, 7]. This enables their real-time detection, either with the aim of correcting erroneous actions of the BCI [8] or with the aim of reducing the possibility of the error reappearing [9, 10].

BCIs that operate in a continuous way have gained attention in the last years because they offer a more natural interaction between user and interface [11, 12, 13]. This has prompted the study of interaction ErrPs during the use of BCIs with continuous control or feedback. Kreilinger et al. [14, 15] investigated the occurrence of interaction ErrPs in a BCI using simultaneously continuous and discrete feedback. Spüler et al. [16] studied interaction ErrPs in a task with continuous control and continuous feedback, given through a cursor, without any additional discrete feedback.

The study of asynchronous detection of ErrPs during continuous movement is still in the early stages. Spüler et al. introduced the asynchronous detection of interaction ErrPs [16]. In the context of an observation task, Omedes et al. asynchronously detected observation ErrPs with sudden and gradually unfolding errors [17, 18]. In the case of gradually unfolding errors, the moment of the error onset was not evident to the observer.

In the current work, we investigate interaction ErrPs with masked and unmasked onset, during a task with continuous control and continuous, jittered and non-jittered, feedback. We consider as unmasked the errors that occur during trials without jittered feedback and as masked the errors that occur during trials with jittered feedback. We hypothesize that masked ErrPs occur later than unmasked ErrPs, when time-locked to the error onset.

MATERIALS AND METHODS

Hardware and data acquisition: EEG data were recorded at 1000 Hz using BrainAmp amplifiers and an actiCap system (Brain Products, Munich, Germany) with 61 active electrodes. The electrodes were placed at positions Fp1, Fp2, AF3, AF4, F7, F5, F3, F1, Fz, F2, F4, F6, F8, FT7, FC5, FC3, FC1, FCz, FC2, FC4, FC6, FT8, T7, C5, C3, C1, Cz, C2, C4, C6, T8, TP9, TP7, CP5, CP3, CP1, CPz, CP2, CP4, CP6, TP8, TP10, P7, P5, P3, P1, Pz, P2, P4, P6, P8, PO9, PO7, PO3, POz, PO4, PO8, PO10, O1, Oz, and O2. The ground electrode was placed at position AFz and the reference electrode was placed on the right mastoid.

 DOI: 10.3217/978-3-85125-533-1-52

Experiment overview: Eight subjects, 5 male, with ages between 19 and 27, participated in the experiment after reading and signing an informed consent form. The experiment consisted of 12 blocks with 30 trials each. Each trial lasted on average 4.6 s. Between the trials, subjects were given 2.5 s to rest. Between the blocks, subjects were allowed to rest for as long as they needed. One third of the trials of each block were randomly assigned as *error trials*, described below. Half of the blocks, randomly selected, consisted of trials with *jittered feedback*, also described below.

Trial and task description: In the beginning of each trial, 4 equally spaced squares were displayed on the upper part of a computer's screen, at the same distance from its centre. One of the squares was randomly chosen to be the target and colored yellow, whilst the others were blue. On the lower part of the screen was a red circle, which represented the cursor (see Fig. 1).

The task consisted in moving the cursor from its initial position to the target with a joystick. The joystick's displacement from its resting position controlled the direction of the cursor's displacement, which moved at constant velocity. The cursor was only allowed to move inside the grey area. A trial ended when the cursor reached the target or when it hit the boundary of the grey region.

In order to minimise eye movements during the trials, the participants were instructed to fixate their gaze on the target at the beginning of each trial, and to start moving the joystick afterwards [19].

Error trials: In these trials, the subject lost the control of the cursor when it was located at a randomly assigned distance from the center of the screen, within the area delimited by the green half-circles depicted in Fig. 1. When this happened, the cursor moved perpendicularly to its direction at the moment of the error onset, until the trial ended. The side to which it deviated was randomly assigned.

Subjects were instructed to keep their gaze fixed on the target and to bring the joystick back to the resting position when recognising that the control over the cursor was lost.

Jittered feedback: With the intention of masking the onset of the errors, in these trials the cursor jittered perpendicularly to the direction of the movement.

Preprocessing: The data were resampled from 1000 Hz to 250 Hz for the electrophysiological analyses and to 25 Hz for the time-locked classification. In addition, a Butterworth filter of order 4 was applied to bandpass the data between 1 and 10 Hz. Then the data were segmented into correct and error trials. To epoch the correct trials, we considered the trials in which the participants successfully guided the cursor to the target and extracted a 1.5 s interval beginning with the cursor crossing the horizontal midline of the screen depicted in Fig. 1. The error trials were segmented using a 1.5 s interval starting 0.5 s before the error onset. For the electrophysiological results, a CAR filter was additionally applied.

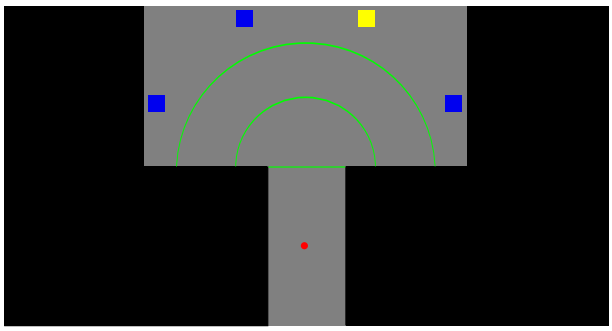

Figure 1: Experimental protocol: a possible setup at the beginning of a trial. The green half-circles delimit the region in which the errors occur. The green horizontal line represents the onset of the correct trials. The green elements are invisible to the subjects.

Outliers rejection: Box-and-whisker diagrams were used to reject outliers [20]. For each channel, the variance of the voltage during correct and error trials was calculated. The lower and upper quartiles, Q1 and Q3, of the channels' variances were used to calculate the interval $[\mathrm{Q1} - k(\mathrm{Q3} - \mathrm{Q1}),\ \mathrm{Q3} + k(\mathrm{Q3} - \mathrm{Q1})]$, with $k = 3$. Channels whose variance lied outside this interval were excluded.

To remove outlier trials, correct and error trials were treated separately. The variance of the voltage at FCz in correct and error trials was used to calculate two intervals, using the procedure described for the channels' rejection. Correct and error trials whose variance of the voltage at FCz lied outside the respective interval were excluded. Additionally, trials whose variance of the voltage at FCz was smaller than 2 µV were also excluded because they reflected problems with the electrode during the recording. On average, 5.64% of the trials were excluded.

Time-locked classification: The raw data were resampled to 25 Hz, bandpass-filtered and segmented as described above. The amplitudes of each channel at each time point of correct and error trials were used as features for training a shrinkage LDA classifier [21], which was tested using 10 times 5-fold cross validation. When classifying correct trials against error trials, training and testing sets were composed of 70% correct trials and 30% error trials. When classifying masked errors against unmasked errors, training and testing sets were balanced.

RESULTS

Electrophysiological analyses: Fig. 2 shows the average signal in error trials (red curve) and correct trials (green curve) at channel FCz for the 8 subjects. The shaded areas represent the 95% confidence interval of the average curves. In the averaged error signal, a sharp negative peak appears at 192 ms after the onset of the error ($t = 0$). It is followed by a pronounced positive peak at 300 ms. Finally, a broader negativity appears, peaking at 592 ms after the error onset. Fig. 2 depicts also the grand

 DOI: 10.3217/978-3-85125-533-1-52

average ErrP (black curve). Fig. 3 depicts the grand average ErrP signal at different scalp positions. Electrodes over the central regions of the scalp show ErrPs with higher peak amplitudes.

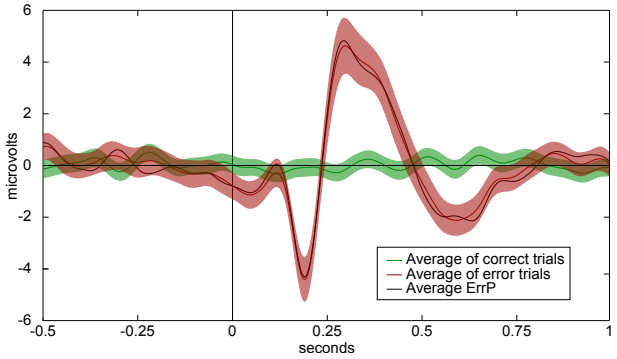

Figure 2: Grand average correct and error signals at channel FCz. The shaded areas represent the 95% confidence interval of the average curves. The black curve represents the grand average ErrP.

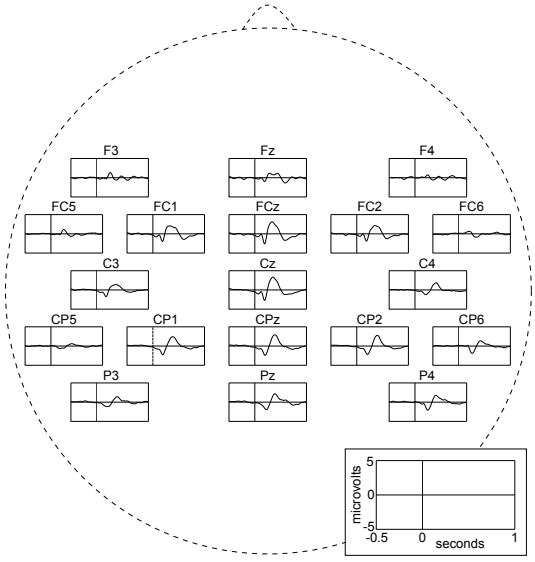

Figure 3: Grand average ErrP at different channels. The diagram on the bottom right indicates the axes' scale of the labeled plots.

Masked and unmasked errors: The grand average correct and error signals, masked and unmasked, are shown in Fig. 4. The averaged unmasked error signal presents a first negative peak 184 ms after the error onset, a positive peak at 316 ms and a broader negativity that peaks at 572 ms. The averaged masked error signal presents a first negative peak at 196 ms, followed by a positive peak at 348 ms and a broader negativity that peaks at 600 ms. The averaged masked error signal is delayed in comparison to the averaged unmasked error signal, when time-locked to the error onset. The peaks of the averaged masked error signal have a lower amplitude than the ones in the averaged unmasked error signal.
Fig. 5 displays the averaged correct and error signals, masked and unmasked, for each subject individually. The first negativity of the grand average error signal, masked and unmasked, is not present in the error signals of all the participants. A delay in the masked error signal in comparison with the unmasked error signal is present in the signals of the majority of the subjects. Subject 5 does not display ErrPs at channel FCz after CAR filtering.

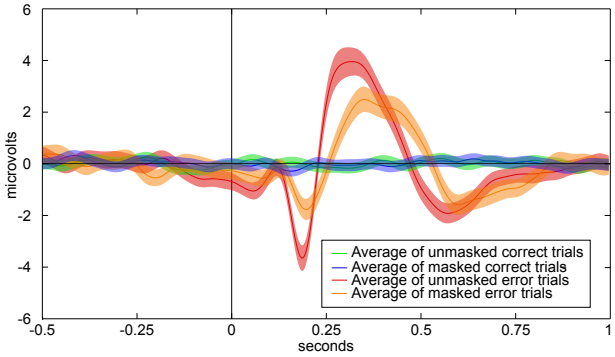

Figure 4: Grand average correct and error signals, masked and unmasked, at channel FCz. The shaded areas represent the 95% confidence interval of the average curves.

Time-locked classification: Both masked and unmasked trials were considered to classify correct trials against error trials. Tab. 1 shows the percentages (mean and standard deviation) of successfully recognised correct and error trials for each subject and their average. Tab. 1 also shows the Cohen-κ coefficient for each subject and their average. We obtained an average of 94.3% recognition rate for correct trials and of 80.3% for error trials. The average Coehen's κ coefficient obtained was of 0.76.
We also tried to classify masked errors against unmasked errors but the results obtained were at chance level (50%), as shown in Tab. 2.

DISCUSSION

We presented results on the electrophysiology of interaction ErrPs and compared errors with masked and unmasked onset. In our study, the ErrP displayed a very similar shape to the error signal because the correct signal was not associated with any event. The masked error signals were delayed in comparison to the unmasked ones, when time-locked to the error onset. We assume that this is due to subjects taking longer to recognise masked errors. The first negative and positive peaks in the masked error signals presented lower amplitudes than in the corresponding peaks in the unmasked error signals. This occurred either due to a variability of the moment in which subjects recognised the error in masked trials or due to

 DOI: 10.3217/978-3-85125-533-1-52

a change in the cursor's direction causing more surprise in unmasked trials than in the masked ones, in which the participants were used to some instability in the feedback.

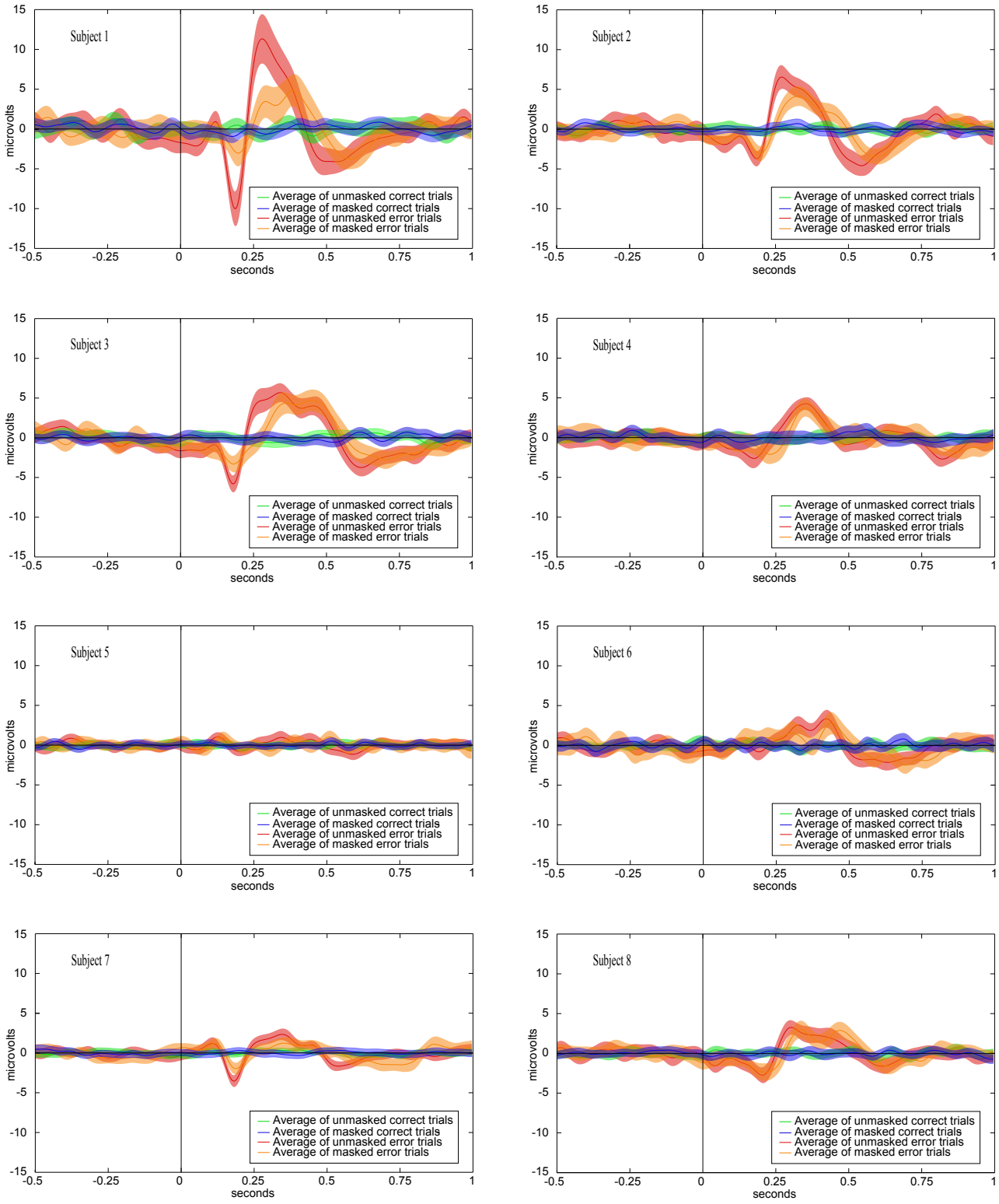

Figure 5: Average of correct and error signals, masked and unmasked, at channel FCz and for each subject. The shaded areas represent the 95% confidence interval of the mean curves.

 DOI: 10.3217/978-3-85125-533-1-52

Table 1: Percentages (mean and standard deviation) of successfully classified correct and error trials and Cohen-κ coefficient.

Subject	Correct (%)	Error (%)	κ
1	98.4 ± 1.4	91.9 ± 5.6	0.91 ± 0.04
2	99.1 ± 1.4	87.5 ± 7.3	0.89 ± 0.06
3	95.0 ± 3.2	81.2 ± 7.1	0.78 ± 0.06
4	93.4 ± 3.2	82.1 ± 8.4	0.76 ± 0.08
5	90.3 ± 4.1	68.7 ± 11.0	0.60 ± 0.12
6	92.0 ± 3.9	77.3 ± 9.9	0.70 ± 0.10
7	92.3 ± 3.8	77.6 ± 10.5	0.71 ± 0.11
8	93.7 ± 3.0	76.1 ± 9.6	0.71 ± 0.09
Average	94.3 ± 4.3	80.3 ± 11.0	0.76 ± 0.13

Table 2: Percentages (mean and standard deviation) of successfully classified masked and unmasked error trials.

Subject	Masked (%)	Unmasked (%)
1	64.9 ± 13.1	68.8 ± 15.7
2	63.2 ± 12.1	54.4 ± 17.6
3	65.8 ± 15.9	70.1 ± 13.6
4	51.3 ± 16.0	62.1 ± 14.1
5	68.4 ± 15.9	68.1 ± 13.4
6	66.4 ± 13.3	55.9 ± 15.3
7	51.0 ± 14.7	55.5 ± 15.3
8	41.9 ± 17.7	41.1 ± 13.8
Average	59.1 ± 17.4	59.5 ± 17.4

CONCLUSION

We investigated interaction ErrPs with masked and unmasked onset. The masked error signals were delayed in comparison to the unmasked ones, when time-locked to the error onset. The first negative and positive peaks in the masked error signals presented lower amplitudes than the corresponding peaks in the unmasked error signals. We obtained good classification rates for correct trials against error trials using time domain features. Nevertheless, our classification results for masked errors against unmasked errors were at chance level.

ACKNOWLEDGEMENTS

The authors would like to thank M.K. Höller for the help during the experiment's preparation. This work was supported by the ERC consolidator grant 681231 "Feel Your Reach".

REFERENCES

[1] Millán JdR, Rupp R, Müller-Putz GR, Murray-Smith R, Giugliemma C, Tangermann M et al. Combining brain—computer interfaces and assistive technologies: State-of-the-art and challenges. Frontiers in Neuroscience, 2010; 4:161.

[2] Hajcak G, Moser JS, Holroyd CB, Simons RF. The feedback-related negativity reflects the binary evaluation of good versus bad outcomes. Biological Psychology, 2006; 71(2):148–154.

[3] Chavarriaga R, Sobolewski A, Millán JdR. Errare machinale est: the use of error-related potentials in brain-machine interfaces. Frontiers in Neuroscience, 2014; 8:208.

[4] Schalk G, Wolpaw JR, McFarland DJ, Pfurtscheller G. EEG-based communication: presence of an error potential. Clinical Neurophysiology, 2000; 111(12):2138–2144.

[5] Ferrez PW, Millán JdR. You are wrong!: Automatic detection of interaction errors from brain waves. In Proc. IJCAI'05, San Francisco, USA, 2005, 1413–1418.

[6] Ferrez PW, Millán JdR. EEG-based brain-computer interaction: Improved accuracy by automatic single-trial error detection. In Proc. NIPS 2007, Vancouver, Canada, 2007, 441–448.

[7] Ferrez PW, Millán JdR. Error-related EEG potentials generated during simulated brain-computer interaction. IEEE Transactions on Biomedical Engineering, 2008; 55(3):923–929.

[8] Ferrez PW, Millán JdR. Simultaneous real-time detection of motor imagery and error-related potentials for improved BCI accuracy. In Proc. of the 4th International Brain-Computer Interface Workshop and Training Course, Graz, Austria, 2008, 197-202.

[9] Blumberg J, Rickert J, Waldert S, Schulze-Bonhage A, Aertsen A, Mehring C. Adaptive classification for brain computer interfaces. In Proc. EMBC 2007, Lyon, France, 2007, 2536–2539.

[10] Llera A, van Gerven MA, Gómez V, Jensen O, Kappen HJ. On the use of interaction error potentials for adaptive brain computer interfaces. Neural Networks, 2011; 24(10):1120–1127.

[11] Galán F, Nuttin M, Lew E, Ferrez PW, Vanacker G, Philips J, Millán JdR. A brain-actuated wheelchair: Asynchronous and non-invasive brain—computer interfaces for continuous control of robots. Clinical Neurophysiology, 2008; 119(9):2159–2169.

[12] Kreilinger A, Kaiser V, Rohm M, Rupp R, Müller-Putz GR. BCI and FES training of a spinal cord injured end-user to control a neuroprosthesis. Biomed Tech, 2013; 58.

[13] Doud AJ, Lucas JP, Pisansky MT, He B. Continuous three-dimensional control of a virtual helicopter using a motor imagery based brain-computer interface. PloS one, 2011; 6(10):1–10.

[14] Kreilinger A, Neuper C, Müller-Putz GR. Error potential detection during continuous movement of an artificial arm controlled by brain–computer interface. Med Biol Eng Comput, 2012; 50(3):223–230.

 DOI: 10.3217/978-3-85125-533-1-52

[15] Kreilinger A, Hiebel H, Müller-Putz GR. Single versus multiple events error potential detection in a BCI-controlled car game with continuous and discrete feedback. IEEE Transactions on Biomedical Engineering, 2016; 63(3):519–529.

[16] M. Spüler, C. Niethammer. Error-related potentials during continuous feedback: using EEG to detect errors of different type and severity. Frontiers in Human Neuroscience, 2015; 9:155.

[17] Omedes J, Iturrate I, Chavarriaga R, Montesano L. Asynchronous decoding of error potentials during the monitoring of a reaching task. In Proc. SMC2015, Hong Kong, China, 2015, 3116–3121.

[18] Omedes J, Iturrate I, Minguez J, Montesano L. Analysis and asynchronous detection of gradually unfolding errors during monitoring tasks. Journal of Neural Engineering, 2015; 12(5):056001.

[19] Sailer U, Flanagan JR, Johansson RS. Eye–hand coordination during learning of a novel visuomotor task. Journal of Neuroscience, 2005; 25(39):8833–8842.

[20] Tukey JW. Exploratory Data Analysis: Past, Present, and Future. Princeton University, Princeton, USA (1993).

[21] Peck R, Van Ness J. The use of shrinkage estimators in linear discriminant analysis. IEEE Trans. Pattern Anal. Mach. Intell.,1982; 4(5):530–537.